The EMBO Journal (2007) 26, 4501–4513 | © 2007 European Molecular Biology Organization | All Rights Reserved 0261-4189/07
www.embojournal.org

THE EMBO JOURNAL

Phosphorylation of Bem2p and Bem3p may contribute to local activation of Cdc42p at bud emergence

Michèle Knaus[1], Marie-Pierre Pelli-Gulli[2,3], Frank van Drogen[1], Sander Springer[2], Malika Jaquenoud[1,3] and Matthias Peter[1,*]

[1]Swiss Federal Institute of Technology (ETH), Institute of Biochemistry, ETH Hönggerberg HPM G 6.2, Zürich, Switzerland and [2]Swiss Institute for Experimental Cancer Research (ISREC), Chemin des Boveresses 155, Epalinges/VD, Switzerland

Site-specific activation of the Rho-type GTPase Cdc42p is critical for the establishment of cell polarity. Here we investigated the role and regulation of the GTPase-activating enzymes (GAPs) Bem2p and Bem3p for Cdc42p activation and actin polarization at bud emergence in *Saccharomyces cerevisiae*. Bem2p and Bem3p are localized throughout the cytoplasm and the cell cortex in unbudded G1 cells, but accumulate at sites of polarization after bud emergence. Inactivation of Bem2p results in hyperactivation of Cdc42p and polarization toward multiple sites. Bem2p and Bem3p are hyperphosphorylated at bud emergence most likely by the Cdc28p-Cln2p kinase. This phosphorylation appears to inhibit their GAP activity *in vivo*, as non-phosphorylatable Bem3p mutants are hyperactive and interfere with Cdc42p activation. Taken together, our results indicate that Bem2p and Bem3p may function as global inhibitors of Cdc42p activation during G1, and their inactivation by the Cdc28p/Cln kinase contributes to site-specific activation of Cdc42p at bud emergence.

The EMBO Journal (2007) **26,** 4501–4513. doi:10.1038/sj.emboj.7601873; Published online 4 October 2007
Subject Categories: signal transduction; cell cycle
Keywords: bud emergence; Cdc28p; Cdc42p; cell polarity; Cln2p

Introduction

The establishment of asymmetry or cell polarity is critical for many biological processes in both single- and multicellular organisms, including cell migration, differentiation, proliferation and morphogenesis (Drubin, 2000). Understanding how cellular components can generate asymmetry represents a key step toward understanding the molecular basis of cellular organization. The polarized assembly of the actin and microtubule cytoskeleton is controlled by Rho-type GTPases, but little is known about their spatial and temporal regulation.

The yeast *Saccharomyces cerevisiae* has proven to be a useful and genetically tractable model organism to study the biochemical pathways leading to the establishment of cell polarity (Pruyne and Bretscher, 2000; Chang and Peter, 2003). Central to the initiation of actin polarization during mating and budding is the local activation of the GTPase Cdc42p by its sole GEF Cdc24p (Johnson, 1999; Pruyne and Bretscher, 2000). In haploid cells, Cdc24p is sequestered in the nucleus during the G1-phase of the cell cycle by binding to the adapter Far1p (Toenjes *et al*, 1999; Nern and Arkowitz, 2000; Shimada *et al*, 2000). In response to mating pheromones, Far1p is exported into the cytoplasm (Blondel *et al*, 1999) and recruits Cdc24p to the site of polarization by binding to Gβγ associated with activated pheromone receptors (Chang and Peter, 2003). During budding, phosphorylation of Far1p by Cdc28p-Cln triggers its ubiquitin-dependent degradation (Henchoz *et al*, 1997), allowing Cdc24p to interact with the small GTPase Rsr1p/Bud1p at the incipient bud site (Kang *et al*, 2001; Shimada *et al*, 2004. In both situations, membrane-recruited Cdc24p is stabilized by the adaptor protein Bem1p, which is involved in a positive feedback loop to keep activated Cdc24p at the sites of polarized growth (Butty *et al*, 2002; Irazoqui *et al*, 2003). Finally, polarized actin cables may further stabilize the axis of polarity by concentrating components involved in Cdc42p activation and surface growth. While these mechanisms promote the formation of a stable polarity axis by site-specific activation of Cdc42p, most models also predict negative mechanisms that ensure global inhibition of Cdc42p activity at the cortex (Levchenko and Iglesias, 2002; Sohrmann and Peter, 2003; Wedlich-Soldner and Li, 2003). Indeed, cells expressing a fast exchanging, mutant form of Cdc42p simultaneously polarize toward multiple sites at bud emergence (Zhang *et al*, 1999), implying that unknown inhibitory mechanisms may prevent Cdc42p activation at the cortex.

GTPase-activating proteins (GAPs) promote intrinsic GTPase activity and thereby negatively regulate Rho-type GTPases (Moon and Zheng, 2003). This mechanism requires a conserved arginine residue (called arginine finger), which interacts with the γ-phosphate of bound GTP thereby triggering its hydrolysis (Bourne, 1997; Rittinger *et al*, 1997). Bem2p, Bem3p, Rga1p and Rga2p have previously been implicated in Cdc42p regulation *in vivo* (Johnson, 1999; Pruyne and Bretscher, 2000), and the GAP domains of Bem2p (Kim *et al*, 1994; Peterson *et al*, 1994), Rga1p and Bem3p (Zheng *et al*, 1993; Gladfelter *et al*, 2002; Smith *et al*, 2002) possess activity toward Rho1p and Cdc42p *in vitro*. Cells singly deleted for any one of these GAPs are viable (Zheng *et al*, 1994; Wang and Bretscher, 1995), but *rga1*Δ *bem3*Δ double mutants show aberrant bud morphology (Smith *et al*, 2002; Caviston *et al*, 2003). These results suggest

*Corresponding author. Swiss Federal Institute of Technology (ETH), Institute of Biochemistry, ETH Hönggerberg HPM G 6.2, Zürich 8093, Switzerland. Tel.: +41 44 633 6586; Fax: +41 44 632 1298;
E-mail: matthias.peter@bc.biol.ethz.ch
[3]Present address: Department of Biochemistry, University of Fribourg, Fribourg 1700, Switzerland

Received: 1 March 2007; accepted: 10 September 2007; published online: 4 October 2007

that some yeast GAPs for Rho-type GTPases exhibit at least partially overlapping functions, but little is known about their regulation *in vivo*. Interestingly, a large-scale study identified Bem3p as a likely target for the cyclin-dependent kinase Cdc28p (Ubersax *et al*, 2003) and likewise Rga2p was recently shown to be phosphorylated by Cdk1 (McCusker *et al*, 2007) and Pho85p/Pcl2p (Sopko *et al*, 2007). These data suggest that the function of Bem3p, Rga2p and perhaps other Rho GAPs might be regulated by phosphorylation, which is further supported by the fact that several mammalian GAPs were found to be phosphorylated *in vivo* (Bernards and Settleman, 2004).

The aim of this study was to identify negative regulators that spatially restrict Cdc42p activation during cellular polarization. Interestingly, we found that Bem2p is required to prevent premature Cdc42p activation during the G1-phase of the cell cycle. Our results suggest that phosphorylation of Bem2p and Bem3p by Cdc28p-Cln2p may inhibit their activity *in vivo*, thereby promoting Cdc42p activation at bud emergence.

Results

bem2Δ cells activate Cdc24p at multiple sites at bud emergence

To investigate how activation of Cdc42p is restricted to a single cortical site at bud emergence, we synchronized wild-type and various *bem*-mutant cells expressing Cdc24p-GFP in G1 by nutrient starvation, and analyzed cellular polarization by differential interference (DIC) and green fluorescent protein (GFP) microscopy. We found that *bem2*Δ cells undergo bud emergence with a significant delay, and over 10% of *bem2*Δ cells form two or more buds that are emerging simultaneously (Figure 1A). Moreover, approximately 80% of the *bem2*Δ cells accumulate Cdc24p-GFP at multiple cortical sites, suggesting that Bem2p may be required to restrict Cdc24p activation at bud emergence. In contrast, wild-type and *bem3*Δ cells accumulate Cdc24p-GFP at a single cortical site and no multibudded cells could be observed (Figure 1A). Supporting these results, *bem2*Δ cells showed a significant growth and actin polarization defect, which was slightly accentuated by simultaneous deletion of *BEM3* (Figure 1B). We have previously shown that Cla4p-dependent hyperphosphorylation of Cdc24p (Gulli *et al*, 2000) and degradation of Gic2p (Jaquenoud *et al*, 1998) requires the GTP-bound Cdc42p (Cdc42p-GTP). Interestingly, *bem2*Δ cells accumulate hyperphosphorylated Cdc24p and exhibit reduced Gic2p levels (Figure 1C), consistent with increased levels of activated Cdc42p *in vivo*. In contrast, *bem1*Δ cells arrested with underphosphorylated Cdc24p and low Gic2p levels, as expected (Gulli *et al*, 2000). Indeed, pull-down assays with GST-CRIB beads confirmed that Cdc42p-GTP accumulated in *bem2*Δ cells compared with wild-type and *bem3*Δ cells (Figure 1D). Taken together, these results suggest that Bem2p, and perhaps to a minor extent also Bem3p, may function to restrict Cdc42p activation to a single cortical site in the G1-phase of the cell cycle.

Overexpression of wild-type but not GAP-inactive Bem3p is toxic and may prevent Cdc42p activation at bud emergence

While overexpression of Bem2p from the inducible *GAL1,10* promoter caused only a mild growth defect, overexpression of Bem3p was highly toxic (Figure 2A). To test whether this defect is caused by its GAP activity, we mutated arginine 950 in the catalytic arginine finger to a glycine or lysine residue. Indeed, wild-type cells overexpressing Bem3p-R950G or Bem3p-R950K were viable, although the mutant proteins were expressed at even higher levels compared with the wild-type control (Figure 2A). Analysis of the terminal phenotype revealed that fewer than 5% of cells overexpressing wild-type Bem3p underwent bud emergence and actin polarization, and most cells arrested with a large, unpolarized morphology (Figure 2B). Synchronized release experiments with cells arrested at bud emergence by depletion of the G1-cyclins confirmed that overexpression of wild-type Bem3p delayed actin polarization at bud emergence (Figure 2C). Likewise, overexpression of Bem3p strongly interfered with shmoo formation after α-factor treatment (Figure 2D), suggesting that increased Bem3p activity may specifically interfere with Cdc42p activation. Wild-type Bem3p did not significantly interact with Cdc42p-C188S (Figure 2E), which lacks a functional CAAX motif required for membrane localization. However, strong binding was detectable with the GTP-locked mutant form Cdc42p-Q61L/C188S, consistent with the notion that GAPs bind their target GTPases preferentially in the GTP-bound state. The interaction of Cdc42p-C188S was also strongly enhanced by GAP-inactive Bem3p-R950G, raising the possibility that inactive Bem3p may form a more stable complex with Cdc42p. In contrast to vector controls, over 80% of wild-type cells overexpressing GFP-Bem3p-R950G accumulated with greatly elongated and hyperpolarized buds (Figure 2B), a morphology which resembles cells lacking GAP activity of Bem3p and Rga1p (Smith *et al*, 2002; Caviston *et al*, 2003). Together, these results suggest that overexpression of Bem3p interferes with Cdc42p activation at bud emergence, while Bem3p-R950G may function in a dominant-negative manner and block GAP activity during bud growth.

Preventing GAP function is sufficient to induce actin polarization in G1-arrested cells

To test whether GAP activity may prevent premature Cdc42p activation and cellular polarization during G1, we arrested YMG258 cells before bud emergence by depletion of the G1-cyclins, and induced the expression of GFP-tagged wild-type Bem3p or the dominant-negative Bem3p-R950G mutant. After 3 h, cellular polarization and bud emergence were monitored by GFP and DIC microscopy, and rhodamine–phalloidin staining of the actin cytoskeleton (Figure 3). Similar to expression of the GTP-locked mutant form Cdc42p-G12V (Gulli *et al*, 2000), we found that over 70% of the G1-arrested cells overexpressing Bem3p-R950G polarized their actin cytoskeleton toward a single site, but the cells were unable to undergo bud emergence. In contrast, cells harboring an empty vector control or overexpressing wild-type GFP-Bem3p were unpolarized. Moreover, GFP-Bem3p-R950G accumulated at sites of polarization, whereas wild-type GFP-Bem3p localized to the plasma membrane and throughout the cytoplasm. Finally, YMG258 cells were released from the G1 arrest by the addition of methionine to re-express Cln2p. As expected, cells overexpressing wild-type Bem3p were unable to polarize their actin cytoskeleton after 30 min (lower panels), whereas vector controls or cells overexpressing GFP-Bem3p-R950G polarized their cytoskeleton

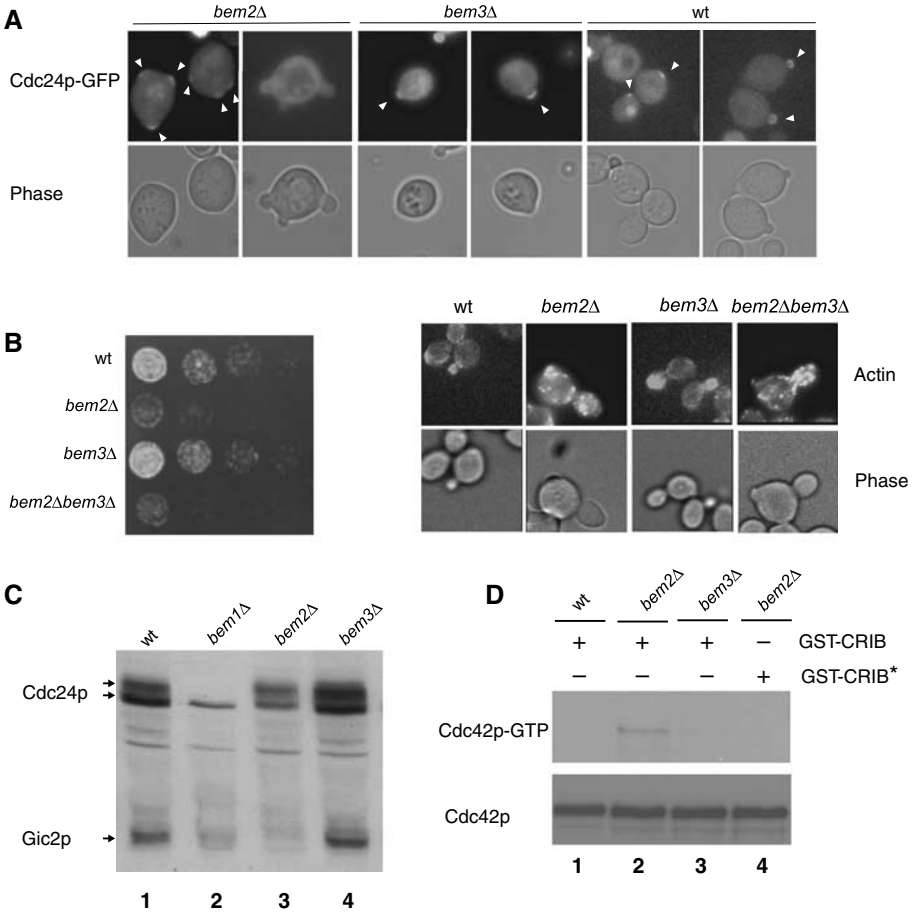

Figure 1 Comparison of Cdc24p-GFP membrane recruitment and Cdc42p activation in wild-type and different *bem*-mutants. (**A**) Cellular morphology and the localization of Cdc24p-GFP (pYS23) was monitored by phase-contrast (lower row) and GFP microscopy (upper row) in wild-type (K699), *bem2*Δ (MPG798) and *bem3*Δ (MPG799) cells released from starvation-induced G1 arrest. Arrowheads mark the localization of Cdc24p-GFP at the sites of polarized growth. (**B**) Five-fold serial dilutions of wild-type (K699), *bem2*Δ (MPG798), *bem3*Δ (YMG799) and *bem2*Δ *bem3*Δ (YMG800) cells were spotted on rich (YPD) media and photographed after 3 days at 25°C. The cellular morphology and polarization state was observed by phase-contrast microscopy (phase) and staining with rhodamine-labeled phalloidin (actin). (**C**) The levels and phosphorylation state of endogenous Cdc24p and Gic2p was analyzed with affinity-purified antibodies in extracts prepared from wild-type (lane 1; BY4741), *bem1*Δ (lane 2; Y03340), *bem2*Δ (lane 3; Y06152) and *bem3*Δ (lane 4; Y02137) cells. (**D**) Extracts prepared from wild-type (BY4741), *bem2*Δ (Y06152) or *bem3*Δ (Y02137) cells were incubated with purified GST-CRIB (lanes 1–3) or the non-binding GST-CRIB* mutant (lane 4) as indicated. Bound Cdc42p (Cdc42p-GTP) was detected with Cdc42p-antibodies (upper panel). Total Cdc42p levels were determined in the extracts (lower panel).

and underwent bud emergence after approximately one hour. Although we do not know the molecular mechanism of the dominant effect of Bem3p-R950G, these results indicate that inactivation of Cdc42p-GAP activity during the G1-phase of the cell cycle may be sufficient to induce cellular polarization possibly by premature activation of Cdc42p.

Bem2p and Bem3p accumulate at the sites of polarized growth and dynamically localize to the plasma membrane in a GAP activity-dependent manner

To examine the subcellular localization of Bem2p and Bem3p during the cell cycle, we expressed fully functional GFP fusions from the inducible *GAL* or the constitutive *ADH* promoter. The localization pattern of Bem3p was confirmed with the GFP fusion expressed from the endogenous promoter (Supplementary Figure 1). Interestingly, both GFP-Bem2p and GFP-Bem3p were cytoplasmic and weakly associated with the plasma membrane during the G1-phase of the cell cycle (Figures 4A and B). Upon cellular polarization, GFP-Bem2p and GFP-Bem3p accumulated at the incipient bud site, and localized predominantly to bud tips and the bud cortex during bud emergence and bud growth (Figure 4A). Coinciding with the switch from polar to isotropic bud growth, GFP-Bem2p concentrated at the mother-bud region (Marquitz *et al*, 2002), while the staining at bud tips weakened. In contrast to previous results with HA-tagged Bem3p (Caviston *et al*, 2003), GFP-Bem3p remained at the cortex of large budded cells, and only localized to the mother-bud region during mitosis. Finally, GFP-Bem2p and GFP-Bem3p accumulated at the tips of mating projections. Interestingly, the cortical localization of GFP-Bem3p during G1 and at bud emergence was prevented by latrunculin-A (LAT-A)-induced disassembly of the actin cytoskeleton (Figure 4C), and GFP-Bem3p instead accumulated in intracellular structures. Likewise, expression of the GTP-locked mutant form Cdc42p-G12V was sufficient to localize GFP-Bem3p to discrete sites at the cortex, and this recruitment was prevented by the addition of LAT-A (data not shown). These results suggest that Bem3p is not stably associated with proteins at the sites of polarized growth, but may be transported to these

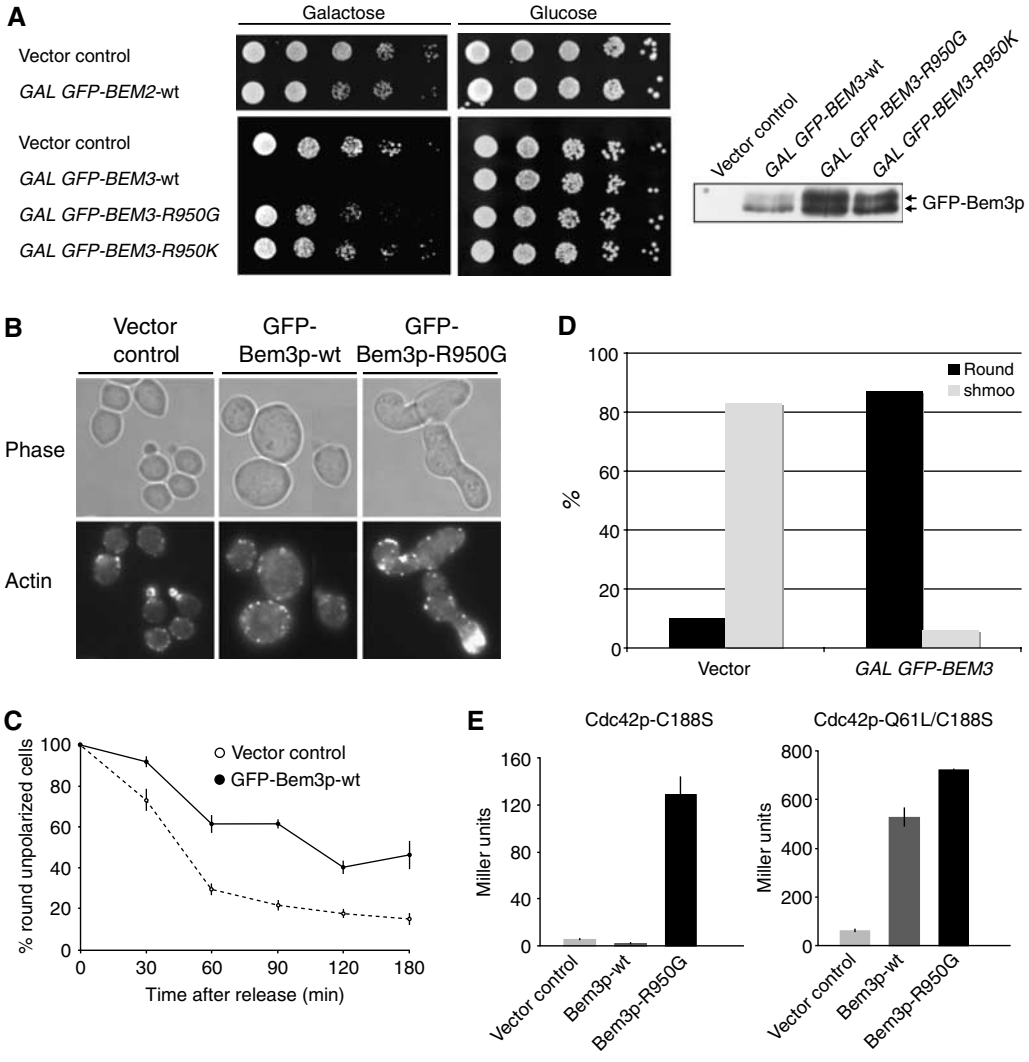

Figure 2 Overexpression of wild-type but not GAP-inactive Bem3p is toxic and may prevent Cdc42p activation at bud emergence. (**A**) Five-fold serial dilutions of wild-type (K699) cells harboring a control vector (pRS415 *GAL1,10*) or plasmids expressing GFP-Bem2p (pMG180), GFP-Bem3p (pYS417), GFP-Bem3p-R950G (pYS418) or GFP-Bem3p-R950K (pYS419) from the inducible *GAL1,10* promoter were spotted on selective media containing 2% galactose (*GAL* promoter on; left plates) or 2% glucose (*GAL* promoter off; right plates). The plates were photographed after 3 days at 30°C. GFP-Bem3p levels were analyzed by immunoblotting with the GFP antibodies of yeast extracts harvested 3 h after induction with 2% galactose (right panel). (**B**) The morphology and actin cytoskeleton of cells harboring an empty control vector (pRS415, *GAL1,10*) or plasmids expressing GFP-Bem3p (pYS417) or GFP-Bem3p-R950G (pYS418) from the inducible *GAL1,10* promoter were analyzed by phase-contrast microscopy (phase, upper panel) or staining with rhodamine-labeled phalloidin (actin, lower panel). Cells were grown to exponential phase and induced with 2% galactose for 18 h. (**C**) *cln1,2,3*ΔΔΔ p*MET-CLN2* cells (yMG258) harboring an empty control vector (pRS415 *GAL1,10*) or a plasmid expressing Bem3p from the inducible *GAL1,10*-promoter (pYS417) were arrested in G1 by the addition of methionine, and Bem3p expression was induced by the addition of 2% galactose for 3 h. The cells were then released and the percentage (%) of round, unpolarized cells was determined microscopically every 30 min. At least 200 cells were counted for each time point. (**D**) Wild-type cells (K699) harboring an empty control plasmid (pRD53) or a plasmid allowing overexpression of Bem3p from the inducible *GAL1,10*-promoter (pYS417) were grown at 30°C in raffinose medium to early log phase. Expression of Bem3p was induced by the addition of galactose (2%) for 3 h before α-factor was added. The percentage (%) of round, unpolarized cells was determined microscopically after 3 h; at least 200 cells were included in the analysis. (**E**) The interaction of wild-type Bem3p (pSS5) and Bem3p-R950G (pMG214) was tested with Cdc42p-C188S (pMG323; left panel) and Cdc42p-Q61L/C188S (pMG362; right panel) by two-hybrid analysis. β-Galactosidase reporter activity is shown as Miller Units, with standard deviations.

sites by an actin-dependent mechanism. Indeed, GFP-Bem3p-containing vesicle-like structures could be visualized in untreated cells by spinning disc microscopy (Figure 4D; Supplementary movies). It appears that these vesicles often emerged from an unknown intracellular compartment (arrow) and rapidly moved to the plasma membrane. FRAP (fluorescence recovery after photobleaching) and iFRAP (inverted FRAP) measurements revealed a half-time of retention for GFP-Bem3p at shmoo tips of approximately 6 s (Figure 4E), indicating that the localization of GFP-Bem3p at sites of polarized growth is transient and highly dynamic.

Bem2p and Bem3p are phosphorylated at bud emergence in a Cdc28p-Cln-dependent manner

To examine the mechanism of the cell-cycle-dependent regulation, we analyzed the expression and phosphorylation state of cells expressing myc-tagged Bem2p and Bem3p at their endogenous locus. First, cells were arrested in G1 by

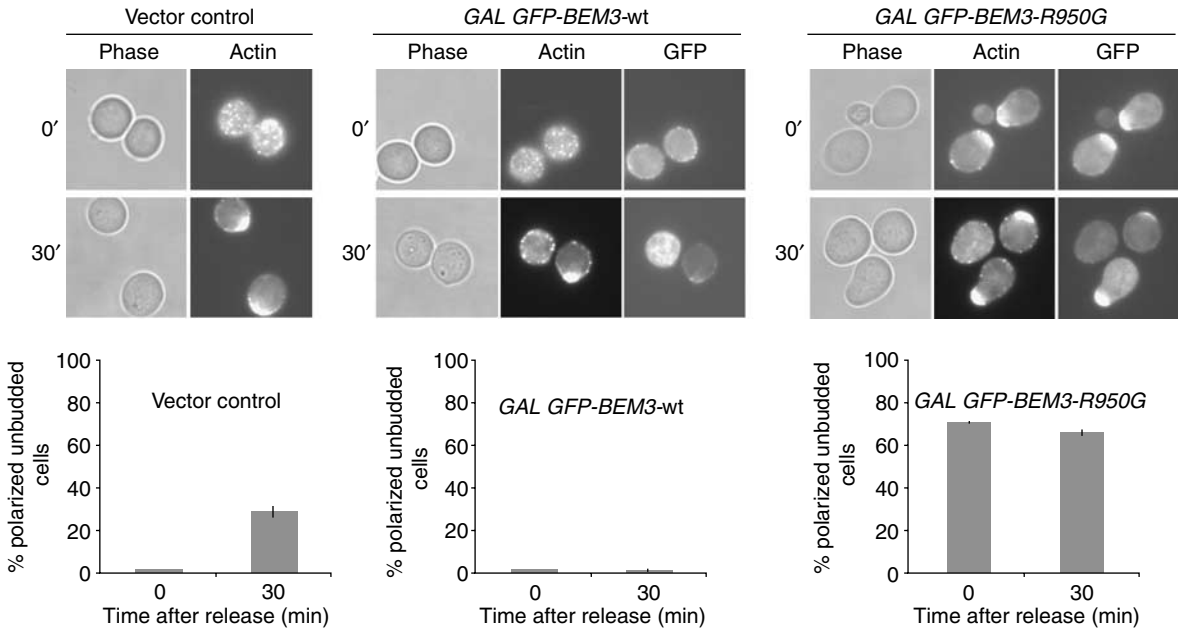

Figure 3 Preventing GAP function is sufficient to induce actin polarization of G1-arrested cells. *cln1,2,3*ΔΔΔ p*MET-CLN2* cells (yMG258) carrying a vector control (pRS415 *GAL1,10*), GFP-Bem3p (pYS417) or GFP-Bem3p-R950G (pYS418) were arrested in G1 by cyclin depletion. The cellular morphology and polarization state were observed by phase-contrast microscopy (phase), staining with rhodamine-labeled phalloidin (actin) and GFP microscopy (GFP) 3 h after induction with 2% galactose (upper row), and 30 min after release from the G1 block (lower row). The number of polarized but unbudded cells was quantified and shown as percentage (%) of the total cells analyzed; at least 300 cells were counted for each time point.

α-factor, in S-phase by hydroxyurea (HU) and in mitosis with nocadazole (Noc) (Figure 5A). In addition, cells were synchronized in G1 either by a α-factor block/release (Figures 5B and C) or G1-cyclin depletion/re-expression protocols (Figure 5D). While Bem2p and Bem3p migrated as slower migrating species when analyzed in G1 cells, both proteins became hyperphosphorylated around bud emergence and Bem3p remained phosphorylated throughout the S and G2/M-phases. Bem3p phosphorylation was not dependent on its catalytic activity, as the Bem3p-R950G- and Bem3p-R950K-mutant proteins were hyperphosphorylated after release from G1 arrest (Figure 5C). In contrast to Cdc24p, Bem3p was efficiently phosphorylated in kinase-inactive *cla4-K594*, *cdc24-5* and *cdc42-6* cells shifted to the restrictive temperature (Figure 5D). Conversely, expression of Cdc42p-G12V was not sufficient to promote Bem3p hyperphosphorylation. Together, these results imply that neither Cla4p nor any other Cdc42p-dependent kinase is required to phosphorylate Bem3p at bud emergence. Finally, Bem2p and Bem3p were phosphorylated in arrested *cdc34-2* cells (Figure 5E), indicating that Cdc28p-Cln rather than Cdc28p-B-type CDKs account for their hyperphosphorylation at bud emergence. Indeed, immunoprecipitated HA-tagged Cln2p was able to phosphorylate *in vitro* an amino-terminal Bem3p fragment (amino acids 1–353) purified form *Escherichia coli* (Figure 5F). Taken together, we conclude that Bem3p and Bem2p may be physiological *in vivo* substrates of the Cdc28p-Cln kinase at bud emergence.

Bem3p is phosphorylated at bud emergence on several sites in its amino-terminal domain

To determine the physiological importance of Bem3p phosphorylation, we immunoprecipitated FLAG-tagged Bem3p from arrested *cdc34-2* cells, and analyzed the phosphorylated peptides by mass spectrometry (MS). This analysis demonstrated that serines 195, 222 and 254 in the amino-terminal domain and serine 880 located close to the catalytic domain of Bem3p were modified by phosphorylation (Figure 6A). All identified phosphorylated serine residues are followed by a proline and thus conform to the minimal CDK consensus site. Although we did not identify serine 585 in our MS analysis, this site conforms to the stringent CDK consensus (Figure 6A) and was thus included in the functional analysis. To corroborate the phosphorylation analysis, we mutated the phosphorylated serines into non-phosphorylatable alanine residues and analyzed the phosphorylation state of the resulting proteins in arrested *cdc34-2* cells (Figure 6B). Bem3p-S3A removes the three sites in the amino-terminal domain (serine 195, 222 and 254), while Bem3p-S5A includes serine 880 and the putative phosphosite 585 outside the catalytic domain of Bem3p (Figure 6A). Indeed, the characteristic slower migrating, phosphorylated forms of Bem3p-S3A and Bem3p-S5A were reduced or absent when analyzed in arrested *cdc34-2* cells (Figure 6B). Together, these data suggest that Bem3p is phosphorylated at bud emergence on serines 195, 222, 254, 880 and possibly 585, most likely by the Cdc28p-Cln2p kinase.

Based on the functional data presented above, we expect that the non-phosphorylatable mutant forms of Bem3p might be hyperactive and thus toxic when expressed in wild-type cells. Indeed, in contrast to wild-type Bem3p, expression of Bem3p-S3A from the endogenous promoter significantly interfered with viability of wild-type cells (Figure 6C) and we were even unable to obtain transformants with pMK81 encoding Bem3p-S5A. Analysis of the cell morphology and actin polarization revealed that almost 40% of the Bem3p-S3A-expressing cells accumulate with an unbudded and unpolarized morphology (Figure 6D). Moreover, approximately 10% of the Bem3p-S3A-expressing cells initiated

actin polarization, but the site was rapidly abandoned at the expense of another site, suggesting that inactivation of Bem3p may also be required after bud emergence to stabilize activated Cdc42p at the sites of polarized growth. Together, these results demonstrate that Bem3p phosphorylation is functionally important to promote cellular polarization and stabilize polar bud growth. To substantiate that non-phosphorylatable Bem3p prevents Cdc42p activation, we expressed wild-type and mutant Bem3p from the weak but regulatable *GALS* promoter (Funk *et al*, 2002). The growth rates of wild-type cells harboring plasmids expressing either wild-type GFP-Bem3p (pMK61), GFP-Bem3p-S3A (pMK70) and GFP-Bem3p-S5A (pMK91) from the *GALS* promoter were indistinguishable when plated on glucose-containing

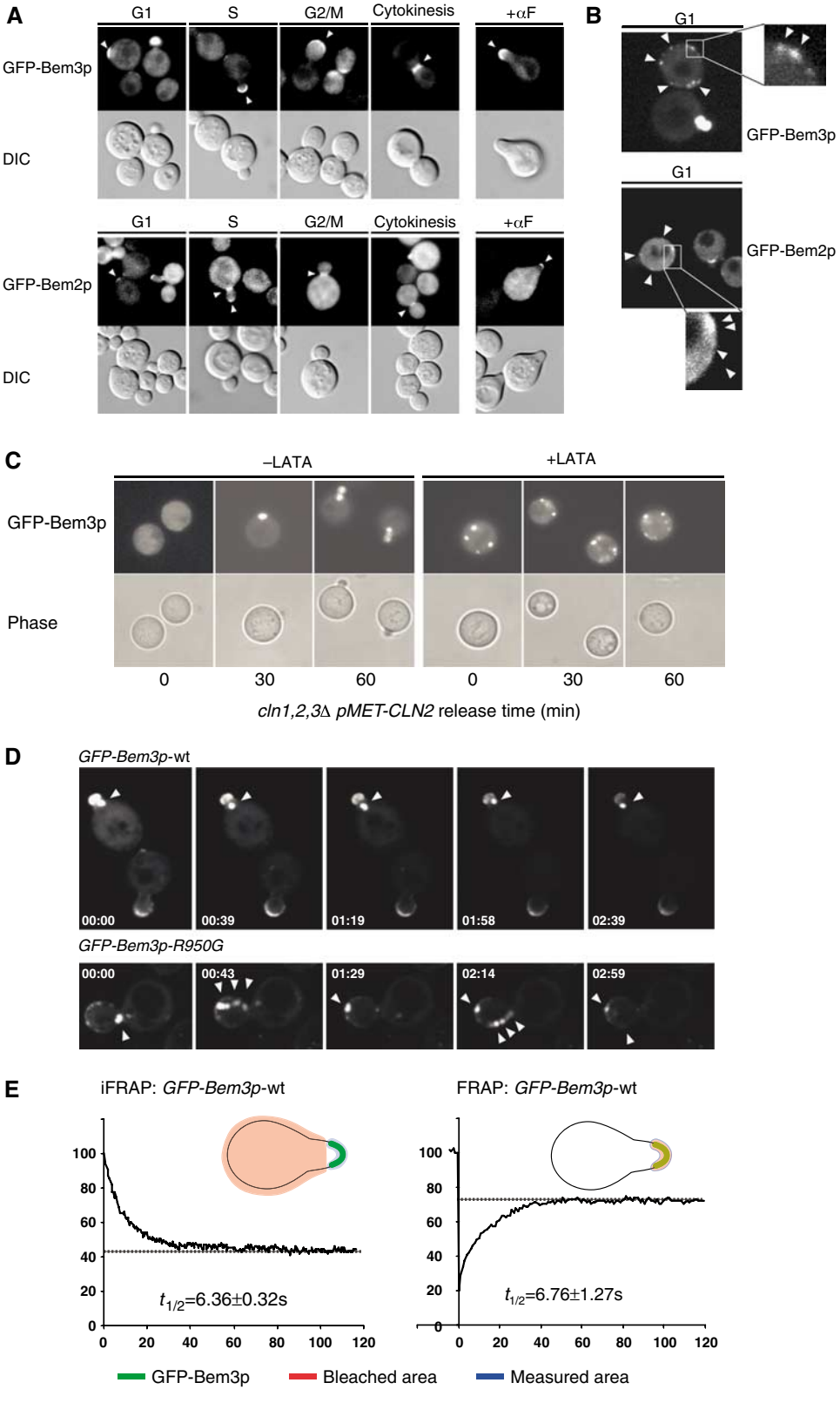

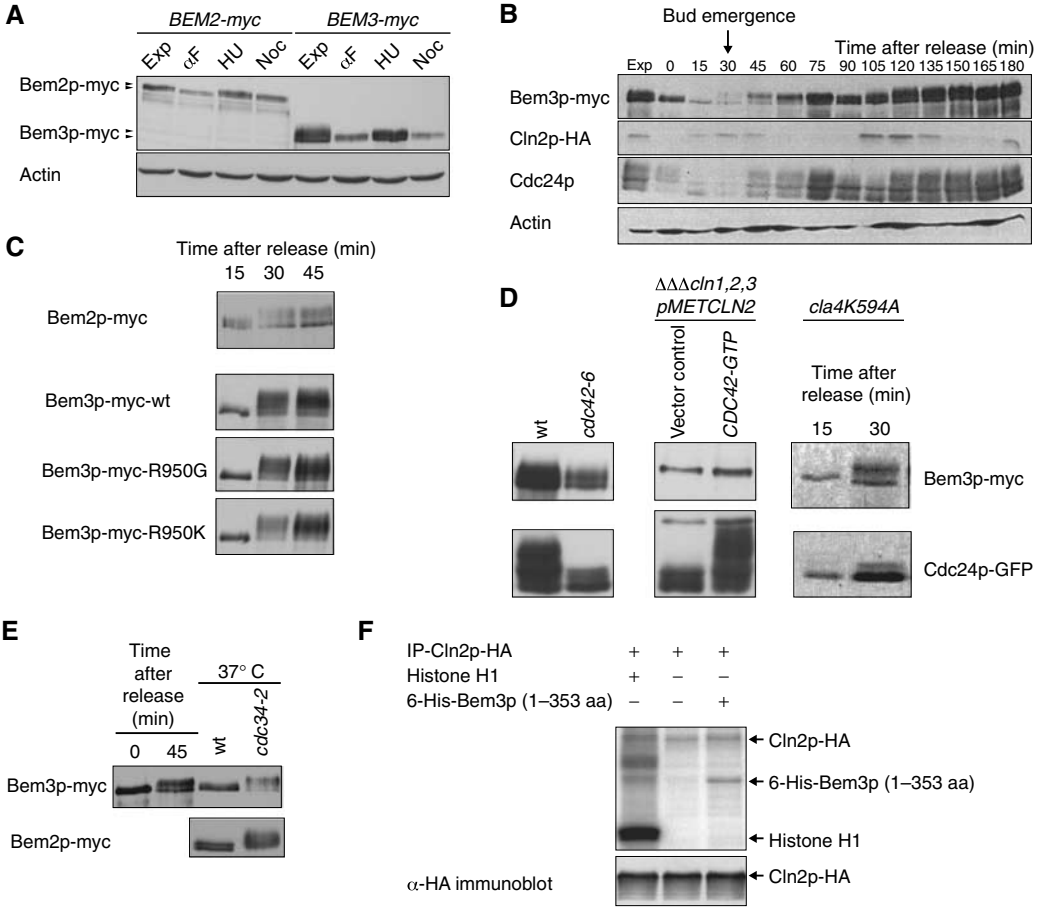

Figure 5 Bem2p and Bem3p are phosphorylated at bud emergence in a Cdc28p-Cln1p/2p-dependent manner. (**A**) Cells expressing Bem2p-myc (yMG769) and Bem3p-myc (pMG779) were grown to exponential phase (exp) and arrested in G1 with α-factor (αF; 8 μg/ml), in S-phase with hydroxyurea (HU; 200 mM) and mitosis with nocodazole (Noc; 15 μg/ml). The protein levels and phosphorylation state of Bem2p-myc and Bem3p-myc were analyzed by immunoblotting with antibodies against the myc epitope. Actin serves as loading control. (**B**) Wild-type (pMG220) cells were synchronized in G1 with α-factor (time 0) and the levels and phosphorylation states of endogenously tagged Bem3p-myc, Cln2p-HA and Cdc24p were analyzed at the times indicated (in minutes) using antibodies specific for the myc and HA epitopes, or with polyclonal antibodies against Cdc24p or actin. The arrow marks the time of bud emergence, which was determined microscopically. (**C**) The phosphorylation state of Bem2p-myc (yMG769), Bem3p-myc (pMG220), Bem3p-R950G-myc (pMG230) and Bem3p-R950K-myc (pMG231) was analyzed by immunoblotting for 15, 30 and 45 min after release from the α-factor arrest. (**D**) The phosphorylation state of Bem3p-myc (pMG220) and Cdc24p was analyzed by immunoblotting of extracts prepared from wild-type (yMG779), *cdc42-6* (yMG796), *cla4K594A* (yMG373) and G1-arrested *cln1,2,3*ΔΔΔ p*MET-CLN2* cells (yMG258) cells expressing mutationally activated Cdc42p-G12V (*CDC42-GTP*). (**E**) The phosphorylation state of Bem2p-myc, Bem3p-myc (pMG220) was analyzed by immunoblotting in wild-type (K699) and *cdc34-2* (yMT670) cells arrested at the G1/S boundary after shifting the cultures to the restrictive temperature (37°C) for 3 h. Wild-type (K699) cells synchronized by α-factor serve as a control for Bem3p phosphorylation. (**F**) Immunoprecipitated Cln2p-HA was incubated with a purified 6-His-tagged amino-terminal fragment of Bem3p (amino acids 1–353) expressed in *E. coli* in the presence of γ^{32}P-labeled ATP. The proteins were separated by SDS–PAGE and phosphorylated proteins visualized by autoradiography (upper panel). Histone H1 serves as positive control for Cdc28p-Cln2p kinase activity. Equal immunoprecipitation of Cln2p-HA was controlled by immunoblotting (lower panel).

Figure 4 GFP-Bem3p and GFP-Bem2p accumulate at distinct cortical sites during G1 and accumulate at the sites of polarized growth during the cell cycle. (**A**) The localization of GFP-Bem3p (pMK61; upper panels) and GFP-Bem2p (pMG180; lower panels) expressed in wild-type (K699) cells from the inducible *GALS and GAL1,10* promoters, respectively, were analyzed by GFP microscopy at different stages of the cell cycle or after α-factor treatment for 2 h (+αF). DIC microscopy (lower rows) shows the morphology of the analyzed cells. Arrowheads mark the localization of the GFP fusion proteins at the cortex. (**B**) The localization of GFP-Bem3p (pMK61) expressed from the inducible *GALS* promoter and GFP-Bem2p (pMG184) expressed from the constitutive *ADH1* promoter was analyzed by spinning-disc confocal microscopy in wild-type (K699) cells during the G1-phase of the cell cycle. Arrowheads mark GFP-Bem3p and GFP-Bem2p localization at the cortex of unpolarized cells. The rectangle shows the area that is magnified × 5 in the inset. (**C**) *cln1,2,3*ΔΔΔ p*MET-CLN2* cells (yMG258) were arrested in G1 by the addition of methionine and Bem3p expression was induced by the addition of 2% galactose for 3 h (time 0). The cells were then released in the presence (+LAT-A; right panels) or absence (−LAT-A; left panels) of the actin depolymerization drug LAT-A and the localization of GFP-Bem3p (upper panels) was monitored by GFP microscopy after the times indicated (in minutes). The morphology of the cells was visualized by phase-contrast microscopy (lower panels). (**D**) The localization of GFP-Bem3p (pMK61) and GFP-Bem3p-R950G (pYS418) in wild-type (K699) cells was visualized by spinning-disc confocal microscopy. Shown are still images of maximal projections of the time-lapse Supplementary movies M1 and M2 at the time points indicated (in minutes; movie window 4 min). The arrowhead marks the intracellular structure that is specifically labelled with GFP-Bem3p. (**E**) The dynamic behavior of GFP-Bem3p at shmoo tips of wild-type (K699) cells was measured by FRAP (right panel) and iFRAP (left panel) as schematically indicated, and blotted in percentage (%) of GFP intensity versus time (in seconds) after photobleaching (time 0). The half-life of recovery (in seconds) was quantified from several independent experiments.

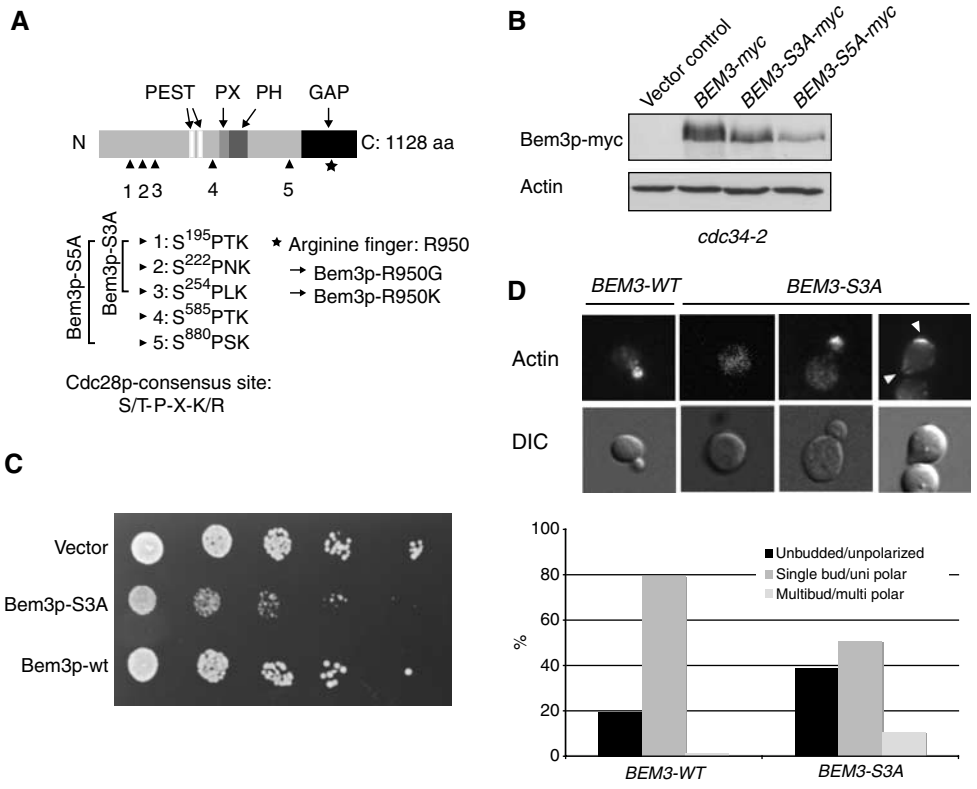

Figure 6 Bem3p is phosphorylated at multiple sites, which are required to inhibit its activity *in vivo*. (**A**) A schematic representation of the domain structure of Bem3p; two PEST motifs (white, aa: 359–385 and aa: 430–451), the phox homology (PX) domain (light gray, aa: 608–621), the pleckstrin homology (PH) domain (dark gray, aa: 633–739) and the GAP domain (black, aa: 927–1097) are highlighted. The arrowheads mark the phosphorylated serine residues, which are mutated in the indicated Bem3p phosphomutants. Serine 585 was not found in the MS analysis, but fulfils the stringent criteria of the consensus sequence established for CDK phosphorylation (S/T-P-X-K/R) and was thus included in the functional analysis (Bem3p-S5A). The asterisks mark the catalytic arginine (R950) located in the GAP domain of Bem3p. (**B**) The phosphorylation pattern of Bem3p-myc (pMG220), Bem3p-S3A-myc (pMK51) and Bem3p-S5A-myc (pMK81) was analyzed by immunoblotting of cell extracts prepared from *cdc34-2* (yMT670) cells shifted for 3 h to the restrictive temperature (37°C). Actin served as control for equal loading. (**C**) Five-fold serial dilutions of an equal number of wild-type (K699) cells transformed with an empty control plasmid (vector, pRS416) or plasmids expressing wild-type (pMG220) or the phosphorylation-deficient Bem3p-S3A mutant (pMK51) from the endogenous promoter. The plates were photographed after 3 days at 30°C. (**D**) Exponentially growing wild-type (K699) cells expressing wild-type Bem3p (pMG220) or Bem3p-S3A (pMK51) from the endogenous promoter were grown to log phase at 30°C. Actin was stained with rhodamine-labeled phalloidin (actin, top row), while DIC microscopy (lower row) shows the morphology of the analyzed cells. Arrowheads mark the localization of polarized actin. The number of cells with an unbudded/unpolarized (black bar), single bud/polarized (dark gray bar) and multibudded/multipolarized (gray bar) morphology were quantified and shown as the percentage (%) of the total cells analyzed; at least 200 cells were counted for each time point.

media (Figure 7A), implying that the promoter is efficiently turned off. As expected, expression of GFP-Bem3p-S5A and to a slightly lesser extent GFP-Bem3p-S3A significantly inhibited growth of wild-type cells on galactose media (Figure 7A), whereas expression of wild-type Bem3p had no effect under these conditions. Moreover, in contrast to wild-type GFP-Bem3p, expression of GFP-Bem3p-S3A and GFP-Bem3p-S5A from the *GALS* promoter was toxic in *cdc24-5* cells grown at the permissive temperature (25°C). This gain-of-function phenotype was abolished by the R950G arginine-finger mutation, demonstrating that Bem3p-GAP activity is required for this effect. Together, these results suggest that phosphorylation of Bem3p is required for viability, most likely by inhibiting its GAP activity to allow site-specific activation of Cdc42p at bud emergence.

To test whether phosphorylation of Bem3p controls its subcellular localization, we expressed GFP-Bem3p, GFP-Bem3p-S3A and GFP-Bem3p-S5A from the *GALS* promoter in wild-type cells. In contrast to GFP-Bem3p, the phosphorylation mutants of GFP-Bem3p were unable to efficiently localize to sites of polarized growth (Figure 7B, and data not shown). However, expression of these mutants also interfered with actin polarization and as a result these proteins accumulated in intracellular structures similar to the localization of GFP-Bem3p in LAT-A-treated cells. Because GAP-inactive GFP-Bem3p-S5A/R950G efficiently accumulated at the sites of polarized growth, we conclude that an intact actin cytoskeleton rather then phosphorylation of Bem3p regulates its polarized localization at bud emergence.

In haploid cells, Cdc28p-Cln2p kinase promotes Cdc42p activation in part by phosphorylating nuclear Far1p, thereby releasing sequestered Cdc24p from the nucleus (Toenjes *et al*, 1999; Nern and Arkowitz, 2000; Shimada *et al*, 2000). Because cells expressing a non-phosphorylatable Far1p-22 mutant from the *ADH* promoter are viable (Henchoz *et al*, 1997), we tested whether Cdc28p-Cln kinase needs to phosphorylate both Far1p and Bem3p to allow efficient bud emergence and Cdc42p activation. Indeed, wild-type cells were unable to grow in the presence of Far1p-22 and GFP-Bem3p-S3A or GFP-Bem3p-S5A (Figure 7C), and arrested as

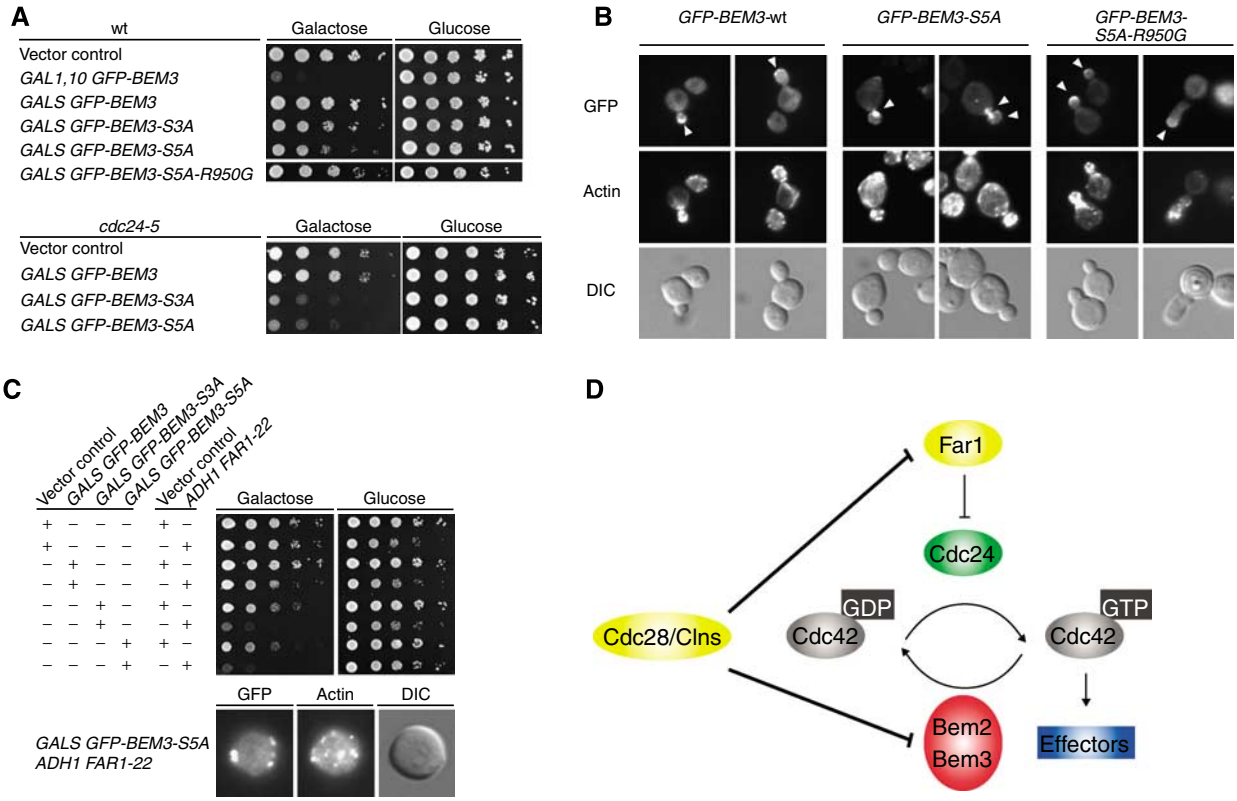

Figure 7 Phosphorylation of Bem3p contributes to cellular polarization at bud emergence, but does not regulate its polarized localization. (**A**) Five-fold serial dilutions of an equal number of wild-type (upper panel; K699) or *cdc24-5* (lower panel; yMG313) cells transformed with a control vector (pRS415, *GAL1,10*) or plasmids allowing as indicated overexpression of GFP-Bem3p (pYS417 and pMK61), GFP-Bem3p-S3A (pMK70), Bem3p-S5A (pMK91), GFP-Bem3p-R950G (pYS418) or GFP-Bem3p-S5A-R950G (pMK101) from the inducible *GAL1,10* or *GALS* promoter, were spotted on media containing galactose (*GAL* promoter on) or glucose (*GAL* promoter off). The plates were photographed after 3 days at 25°C. (**B**) The localization of GFP-Bem3p (pMK61), GFP-Bem3p-5A (pMK91) and GFP-Bem3p-5A-R950G (pMK101) expressed in wild-type (K699) cells from the inducible *GALS* or *GAL1,10* promoter, respectively, was analyzed by GFP microscopy (upper row). Polarized actin was stained with rhodamine-labeled phalloidin (actin, middle row), and DIC microscopy (lower row) shows the morphology of the analyzed cells. Arrowheads mark the localization of the GFP fusion proteins at tips of small buds. (**C**) Five-fold serial dilutions of an equal number of wild-type (K699) cells transformed with a combination of plasmids allowing as indicated overexpression of GFP-Bem3p (pYS417), GFP-Bem3p-S3A (pMK70) or GFP-Bem3p-S5A (pMK91) from the inducible *GALS* and Far1p-22 (pYS82) from the *ADH1* promoter (or respective control vectors). The cells were spotted on media containing galactose (*GAL* promoter on) or glucose (*GAL* promoter off) and photographed after 3 days at 25°C. (**D**) We propose that the Cdc42p-GAPs Bem2p and Bem3p prevent premature activation of Cdc42p during the G1-phase of the cell cycle. Upon cellular polarization, the G1-CDK Cdc28p/Cln phosphorylates and inhibits Bem2p and Bem3p activity, thereby promoting the formation of a stable polarity axis by lowering the threshold for Cdc42p activation. In haploid cells, Cdc28p/Clnp also triggers degradation of nuclear Far1p, thereby releasing Cdc24p into the cytoplasm. Cdc28p-Cln kinase thus promotes bud emergence by phosphorylating both positive and negative regulators of Cdc42p.

large unbudded cells with an unpolarized actin cytoskeleton. These results suggest that Cdc28p-Cln inactivates two distinct inhibitory pathways to allow site-specific activation of Cdc42p at bud emergence.

Discussion

In this study, we provide evidence that the Cdc42p GAPs Bem2p and Bem3p are regulated by the Cdc28p-Cln1/2p kinase to promote directed actin polymerization at bud emergence. Bem2p and Bem3p may dynamically localize at the cell cortex in the G1-phase of the cell cycle, and prevent premature Cdc42p activation *in vivo*.

GAP activity may be required in G1 to prevent premature Cdc42p activation

Our results suggest that the Cdc42p GAP Bem2p may prevent premature activation of Cdc42p during the G1-phase of the cell cycle. In support of this notion, synchronized *bem2*Δ cells exhibit increased levels of Cdc42p-GTP and polarize simultaneously toward multiple sites. Conversely, overexpression of Bem2p is able to suppress the toxic effects of a constitutively active Cdc24p mutant (Shimada *et al*, 2004). Although Bem2p appears to exert the greatest effect on Cdc42p activation at bud emergence, it is likely that other members of the Rho-GAP family including Bem3p and Rga2p contribute to this regulation (Smith *et al*, 2002; Sopko *et al*, 2007). Indeed, overexpression of wild-type Bem3p or expression of non-phosphorylatable Bem3p mutants from the endogenous promoter interferes with Cdc42p activation at bud emergence, while conversely, expression of dominant-negative Bem3p-R950G in unpolarized G1 cells is sufficient to trigger polarization of the actin cytoskeleton. Finally, Bem2p and Bem3p are underphosphorylated during G1, but become hyperphosphorylated *in vivo* concomitant with bud emergence. These results suggest that the activity of Bem2p and possibly Bem3p is required to prevent spontaneous activation of Cdc42p during the G1-phase of the cell cycle, while their

inactivation is needed to lower the threshold for Cdc42p at bud emergence (Figure 7D).

Cdc28p-Cln2p kinase may promote bud emergence by inhibiting the activity of the Cdc42p-GAPs Bem3p and possibly Bem2p

In haploid G1 cells, phosphorylation of nuclear Far1p by Cdc28p-Cln triggers its degradation, thereby releasing Cdc24p into the cytoplasm. However, cytoplasmic Cdc24p is not sufficient to initiate bud emergence (Gulli *et al*, 2000), implying that additional substrates must exist to cause site-specific activation of Cdc42p. Interestingly, combining non-phosphorylatable mutants of Bem3p with a non-degradable Far1p mutant is toxic and the cells fail to polarize their actin cytoskeleton. Our results suggest that Bem3p and possibly Bem2p are inactivated at bud emergence by Cdc28p-Cln kinase (Figure 7D). First, phosphorylation of Bem3p *in vivo* is dependent on Cdc28p-Cln activity, but does not require Cdc42p activation or the Cdc42p-Cla4p negative feedback loop. Second, Bem3p is phosphorylated by Cdc28p-Cln2p kinase *in vitro* and the phosphorylated serine residues conform to the known CDK consensus site. Finally, expression of a non-phosphorylatable Bem3p at least partially mimics the loss of Cdc28p-Clnp activity with respect to its role in bud emergence. The molecular mechanism of Bem3p inhibition is not clear, but does not directly affect its subcellular localization. Most of the phosphorylation sites are clustered within the amino-terminal domain and only one is located close to the catalytic domain itself. In analogy to several protein kinases, we speculate that the amino-terminus may exert an inhibitory function on its carboxy-terminal GAP domain, which is prevented by multiple phosphorylation. Interestingly, phosphorylation of the Cdc42p-GAP Rga2p by Cdk1 (McCusker *et al*, 2007) and the CDK Pho85p/Pcl2p (Sopko *et al*, 2007) might also inhibit its activity *in vivo*, raising the possibility that inhibition of GAPs by CDK phosphorylation may be a general mechanism.

GAP inactivation may occur asymmetrically during budding and mating

Phosphorylation of Bem2p and Bem3p may occur uniformly throughout the cells, and together with site-specific recruitment and stabilization of Cdc24p allow robust activation of Cdc42p at the incipient bud and mating sites (Chang and Peter, 2003). Consistent with this notion, expression of a dominant-negative Bem3p-R950G mutant in G1-arrested cells results in spontaneous actin polarization possibly by the amplification of stochastic differences in Cdc42p-GTP levels by positive feedback loops. However, it is tempting to speculate that at least in some cases Bem2p and Bem3p phosphorylation may occur asymmetrically and thereby contribute to the formation of a stable polarity axis. Although Cln2p is predominantly cytoplasmic, it transiently accumulates at bud sites (unpublished observations) and may therefore preferentially inhibit the Cdc42p GAPs at the sites of polarization. A more striking example of asymmetric kinase activation is observed during yeast mating; the MAP kinase Fus3p is activated specifically at shmoo tips by binding to its scaffold Ste5p at the sites of engaged pheromone receptors (Elion, 1995). Although it is not clear whether Fus3p is able to phosphorylate Bem2p and Bem3p in response to pheromones, many CDK sites are also phosphorylated by MAP kinases *in vitro* and *in vivo* (Peter *et al*, 1992). As activated Fus3p rapidly dissociates from Ste5p (van Drogen *et al*, 2001), it may create an asymmetric distribution of Bem2p/Bem3p phosphorylation and thereby establish a graded threshold of Cdc42p activation, with the minimum at shmoo tips. Consistent with this model, *bem2*Δ cells are unable to form a single mating projection in response to pheromones. Mathematical models of chemotactic systems postulated a global and diffusible inhibitory signal (Levchenko and Iglesias, 2002; Sohrmann and Peter, 2003), and we speculate that local inhibition of Cdc42p-GAPs may contribute to directed polarization in particular at early stages of polarization. Interestingly, recent work also revealed an actin-dependent negative feedback loop that destabilizes the polarity axis (Ozbudak *et al*, 2005). Deletion of individual Cdc42p-GAPs stabilized the dynamic behavior of the polarization site, suggesting that targeted delivery of GAPs together with local inhibition may promote the establishment and maintenance of the polarity axis along the pheromone gradient.

Bem2p and Bem3p may also function after bud emergence

While Cdc28p-Cln kinases inhibit Bem3p at bud emergence, Cdc28p-Clb-type CDKs at least partially maintain this phosphorylation pattern, implying that Bem3p may be inactive during the S and G2-phases of the cell cycle. Indeed, expressing the phosphorylation-compromised Bem3p-S3A mutant from the endogenous promoter not only interferes with cellular polarization at bud emergence, but also later in the cell cycle, suggesting that continued phosphorylation of Bem3p is necessary to prevent its misregulation. Cdk1 has been shown to control bud growth after bud emergence by phosphorylating components associated with Cdc24p (McCusker *et al*, 2007). However, cells overexpressing dominant-negative Bem3p-R950G accumulate with hyperpolarized buds, implying that GAP activity may also be needed later in the cell cycle. GFP-Bem3p accumulates at the tips of small buds and mating projections (Caviston *et al*, 2003) and may thus contribute to Cdc42p inactivation at the sites of polarized growth. FRAP and iFRAP analyses showed that GFP-Bem3p at these sites is highly dynamic, with a half-time of recovery of a few seconds. Internalized Bem3p accumulates within an internal compartment and in vesicle-like structures, which rapidly move toward bud tips. Based on the speed of individual vesicles it is likely that they are transported by myosin motors along linear actin tracks, and LAT-A experiments confirm that the polarized localization of GFP-Bem3p is dependent on an intact actin cytoskeleton. Like Bem3p, GFP-Bem2p is found at the sites of polarized growth, but Bem2p and Bem3p may also perform specific functions at distinct subcellular sites. For example, GFP-Bem2p accumulates at the mother-bud neck during S-phase, while GFP-Bem3p remains at the bud tips and is only found at the mother-bud neck region during cytokinesis. Bem2p regulates the dynamics of septin assembly during cytokinesis (Caviston *et al*, 2003) most likely by promoting rapid cycling of GTP–GDP exchange on Cdc42p. Moreover, Bem2p triggers the morphogenesis checkpoint by a GAP-independent mechanism (Marquitz *et al*, 2002). Although Bem2p and Bem3p possess GAP activity toward Cdc42p *in vitro*, they may also use other Rho-type GTPases as substrates (Zheng *et al*, 1993).

Thus, although Bem2p and Bem3p are important to prevent Cdc42p activation before bud emergence, it is possible that they may also regulate other Rho-type GTPases.

Materials and methods

Strain constructions and genetic manipulations

Yeast strains are described in Table I. The genotypes of the yeast strains are as follows: W303 (*ade2-1*, *trp1-1*, *can1-100*, *leu2-3,112*, *his3-11,15*, *ura3*, *ssd1-d2*) and S288C (*his3Δ1 leu2Δ0 met15Δ0 ura3Δ0*), unless noted otherwise. The yeast k.o. collection was purchased from Euroscarf (S288C background). Gene deletions were obtained by PCR amplification of the respective *KANMX4* cassette with 3′ and 5′ UTR-specific primers, transformation and integration by homologous recombination. Correct deletions were confirmed by resistance to G418 (*KAN*) (200 μg/ml) and PCR. Standard yeast growth conditions and genetic manipulations were used (Guthrie and Fink, 1991).

DNA manipulations and two-hybrid assays

Plasmids are described in Table II. Standard procedures were used for recombinant DNA manipulations and details of plasmid constructions and oligo sequences will be provided upon request. Site-directed mutagenesis was performed by PCR and confirmed by sequencing. Two-hybrid assays were performed in YACB165 containing the LacZ reporter plasmid pSH18.34 (Butty *et al*, 1998). Cells were grown in selective media containing 2% raffinose and induced with 2% galactose for 2 to 3 h. Miller Units are the average of at least three independent colonies, with standard deviations (Brown *et al*, 1997).

Microscopy and morphological examination

Proteins tagged with GFP (S65T variant) were visualized with a Zeiss Axiovert 200M fluorescence microscope equipped with an Orca-ER CCD camera (Hamamatsu, Japan) using the Zeiss GFP filterset no. 10, a Plan-Apochromat $\times 63$ or $\times 100$ objective (NA 1.4) and Openlab software (Improvision, UK). Spinning-disc confocal images were acquired using the same basic microscope setup additionally equipped with a spinning-disc head and an argon laser (458, 488, 514 nm) (Visitec Company, UK). For time-lapse microscopy, z-stacks of 7–9 spinning-disc confocal images separated by 0.2 μm each were taken at 14–15 time points, with less than 10 s intervals between stacks. Z-stacks were maximally projected and converted into QuickTime movie format playing five frames per second. FRAP and iFRAP analyses were performed with a Zeiss LSM510 confocal laser scanning microscope. Photobleaching was applied on the area indicated with the confocal pinhole fully open (optical slice < 7.3 μm). Scans were collected continuously (scan time of 393.21 ms) for a maximum of 120 s using the acquisition software LSM510 (Carl Zeiss MicroImaging Inc.). Bleaching regions were irradiated with two iterations of 100% laser

Table II Plasmid list

Strain	Relevant characteristics	Source or reference
pRS415	*CEN LEU2*	Sikorski and Hieter (1989)
pRS416	*CEN URA3*	Sikorski and Hieter (1989)
pRS426	*2μ URA3*	Sikorski and Hieter (1989)
pEG202/3	*2μ HIS3 ADH1-LexA-DBD*	Gyuris *et al* (1993)
pJG4-5/6	*2μ TRP1 GAL1,10-AD*	Gyuris *et al* (1993)
pRD53	*CEN URA3 GAL1,10*	R Deshaies
pMG180	*pRS416 GAL1,10 GFP-BEM2*	This study
pNP337	*pRS416 GFP-Bem3*	This study
pMG184	*pRS416 ADH1 GFP-BEM2*	This study
pMG220	*pRS416 BEM3-myc*	This study
pMK51	*pRS416 BEM3-S3A-myc*	This study
pMK81	*pRS416 BEM3-S5A-myc*	This study
pMG230	*pRS416 BEM3-R950G-myc*	This study
pMG231	*pRS416 BEM3-R950K-myc*	This study
pYS417	*pRS415 GAL1,10 GFP-BEM3*	This study
pYS418	*pRS415 GAL1,10 GFP-BEM3-R950G*	This study
pYS419	*pRS415 GAL1,10 GFP-BEM3-R950K*	This study
pMK61	*pRS415 GALS GFP-BEM3*	This study
pMK70	*pRS415 GALS GFP-BEM3-S3A*	This study
pMK91	*pRS415 GALS GFP-BEM3-S5A*	This study
pMK101	*pRS415 GAL1,10 GFP-BEM3-5A-R950G*	This study
pMK187	*pRS416 GALS GFP-BEM3*	This study
pYS23	*pRS415 ADH1 CDC24-GFP*	Shimada *et al* (2000)
pMJ383	*pRS314 GAL1,10 GIC2-GFP*	Jaquenoud and Peter (2000)
pMG323	*pEG202 CDC42-C188S*	Butty *et al* (1998)
pMG362	*pEG203 CDC42-Q61L-C188S*	This study
pSS5	*pJG4-6 BEM3*	This study
pMG214	*pJG4-6 BEM3-R950G*	This study
pMG215	*pJG4-6 BEM3-R950K*	This study
pYS82	*pRD53 ADH FAR1-22*	This study
pMG201	*pET30A 6HIS-BEM3 (1-353)*	This study
pMK195	*pRS415 GAL1,10 BEM3-FLAG*	This study

Table I Yeast strain list

Strain	Genotype	Background	Source or reference
K699	*Mata*	W303	K Nasmyth
K700	*Matα*	W303	K Nasmyth
MPG798	*Mata bem2::KANMX4*	W303	This study
MPG799	*Mata bem3::LEU2*	W303	This study
MPG800	*Mata bem3::LEU2 bem2::KANMX4*	W303	This study
BY4741	*Mata*	S288c	Euroscarf
Y03340	*Mata bem1::KANMX4*	S288c	Euroscarf
Y06152	*Mata bem2::KANMX4*	S288c	Euroscarf
Y02137	*Mata bem3::KANMX4*	S288c	Euroscarf
yMG258	*Mata cln1::HisG, cln2Δ, cln3::HisG, YipLac204-MET CLN2*	W303	Gulli *et al* (2000)
yMG373	*Mata cla4 K594A*	W303	D Kellogg
yMG796	*Matα cdc42-6 BEM3-myc::KANMX4*	W303	This study
yMT670	*Mata cdc34-2*	W303	M Tyers
yMG313	*Matα cdc24-5*	W303	Butty *et al* (2002)
yMG769	*Mata BEM2-myc13-HIS3 bar1-1*	W303	This study
yMG779	*Mata BEM3-myc13-HIS3 bar1-1*	W303	This study
yMG792	*Mata cdc34-2 cln2::CLN2-HA3-LEU2*	W303	This study
yMG801	*Mata cdc34-2 BEM3-myc::KANMX4*	W303	This study
YMP1101	*Mata cdc34-2 BEM3-myc::KANMX4*	W303	This study
yMG776	*Mata rga1::HIS3 bem3::TRP1*		G Sprague

intensity at 100% output of an argon laser (488 nm), and scans were collected with 2% laser intensity using the same conditions.

Actin cytoskeletal rearrangements were monitored by staining with rhodamine-labeled phalloidin (Molecular Probes) as described (Jaquenoud *et al*, 1998) and viewed using a Chroma Technology Corp. filterset no. 41002 (TRITC). To determine the budding index, at least 200 cells were counted using DIC or phase-contrast microscopy. Cells were treated with LAT-A (0.2 mM in DMSO) for 30 min at 25°C and actin depolymerization was monitored by staining with rhodamine–phalloidin.

Cell cycle synchronization and in vivo phosphorylation analysis

Exponentially growing cells were arrested in G1 by the addition of 50 μg/ml α-factor (LIPAL-Biochemicals, Zurich), unless otherwise indicated. After 2 h, cells were washed and released into fresh media without α-factor. Samples for protein extracts and budding index determination were taken at the indicated time points. G1 arrest of *cln1,2,3*Δ p*MET-CLN2* (YMG258) cells was achieved by repressing the expression of Cln2p for 3 h in selective medium supplemented with 2 mM methionine. Induction of *GAL-BEM3* and its mutant variants was carried out as described previously (Gulli *et al*, 2000). Cells were washed and released by inducing Cln2p expression in medium lacking methionine. Nutritional synchronization was carried out as described (Jaquenoud and Peter, 2000). To analyze the phosphorylation sites of Bem3p, *cdc34-2* cells (yMT670) expressing FLAG-tagged Bem3p from the *GAL1,10* promoter (pMK195) were grown to logarithmic phase at 25°C in medium containing 2% raffinose. Galactose (2%) was then added for 30 min before the cultures were shifted to 37°C for 90 min. Cells were lysed in Buffer M (50 mM Tris–HCl pH 7.5, 100 mM NaCl, 50 mM NaF, 5 mM EDTA, 1 mM DTT, 0.2 mM PMSF, 10 μg/ml aprotinin, 10 μg/ml leupeptin and 10 μg/ml pepstatin), FLAG-Bem3p was purified using anti-FLAG–sepharose beads, digested and analyzed on an LTQ linear quadrupole ion-trap mass spectrometer. The phosphorylation-indced migration of Bem3p-myc (pMG220), Bem3p-3A-myc (pMK51) and Bem3p-5A-myc (pMK81) was analyzed by immunoblotting of cell extracts prepared from *cdc34-2* cells (yMT670) grown at 25°C in rich medium and arrested before S-phase by shifting the cultures for 3 h to 37°C.

In vitro kinase assays

Yeast cells (yMG792) were lysed in a one-shot at maximal pressure in lysis buffer (50 mM Tris–HCl pH 7.5, 100 mM NaCl, 50 mM NaF, 5 mM EDTA, 1 mM DTT, 1% Triton X-100, 0.2 mM PMSF, 10 μg/ml aprotinin, 10 μg/ml leupeptin and 10 μg/ml pepstatin). Cln2p-HA was immunoprecipitated with anti-HA (12CA5) antibodies bound to PGS beads and washed three times in lysis buffer, twice in kinase buffer (50 mM Tris–HCl pH 7.5, 20 mM $MgCl_2$, 1 mM DTT, 0.5 mM Na_3SO_4, 10 μg/ml aprotinin and 10 μg/ml leupeptin) and twice in kinase buffer containing ATP. Kinase activity was assayed by monitoring the phosphorylation of Histone H1 (Sigma-Aldrich) and *E. coli*-purified 6-His-Bem3p-[1–353] (pMG201). Each reaction contained 2.5 μg substrate, 5 μM ATP, 1 μl ATPγ^{32}P (Amersham Pharmacia; stock at 10 mCi/ml) in kinase buffer. Kinase reactions were incubated at 30°C for 30 min and stopped with the addition of LSB and heat denaturation for 5 min at 95°C. The reactions were resolved by SDS–PAGE, stained with Coomassie blue and developed by autoradiography.

CRIB-binding assays, antibodies and immunoblotting

Binding assays with purified GST-CRIB were performed as described (Gulli *et al*, 2000). Briefly, wild-type or mutant CRIB domains of Gic2p (aa 189–213) fused to GST were purified from *E. coli* on glutathione–Sepharose beads, and incubated for each pull-down reaction with 500 mg of precleared yeast extracts for 30 min at 4°C. The beads were washed three times and bound Cdc42p was eluted with gel loading buffer and visualized by immunoblotting with Cdc42p antibodies. An aliquot of the extract before the binding assay was immunoblotted to determine the total Cdc42p levels.

Standard conditions were used for yeast cell extracts and immunoblotting. Western blotting was performed using α-myc 9E11 (ISREC), α-actin (Roche), α-GFP (B34/8 and C163/8, ISREC), α-HA_{11} (Covance) and α-GST (Santa Cruz Biotechnology Inc.) antibodies. Cdc24p and Gic2p antibodies have been reported previously (Brown *et al*, 1997; Gulli *et al*, 2000), while Cdc42p and Clb2p antibodies were gifts from D Kellogg (UCSC).

Supplementary data

Supplementary data are available at *The EMBO Journal* Online (http://www.embojournal.org).

Acknowledgements

We thank M Tyers, E Bi, D Kellogg, D Lew, G Sprague and Y Barral for providing plasmids, strains and antibodies, and R Sopko and B Andrews for sharing unpublished results. We are grateful to C Rupp for technical assistance and P Wiget and the ETHZ Light Microscopy Center for help with microscopy. We thank members of the Peter and Barral groups for stimulating discussion, and B Andrews and M Sohrmann for critical reading of the manuscript. This work was supported by the Swiss National Science Foundation and the ETH/Zurich.

References

Bernards A, Settleman J (2004) GAP control: regulating the regulators of small GTPases. *Trends Cell Biol* **14:** 377–385

Blondel M, Alepuz PM, Huang LS, Shaham S, Ammerer G, Peter M (1999) Nuclear export of Far1p in response to pheromones requires the export receptor Msn5p/Ste21p. *Genes Dev* **13:** 2284–2300

Bourne HR (1997) G proteins. The arginine finger strikes again. *Nature* **389:** 673–674

Brown JL, Jaquenoud M, Gulli MP, Chant J, Peter M (1997) Novel Cdc42-binding proteins Gic1 and Gic2 control cell polarity in yeast. *Genes Dev* **11:** 2972–2982

Butty AC, Perrinjaquet N, Petit A, Jaquenoud M, Segall JE, Hofmann K, Zwahlen C, Peter M (2002) A positive feedback loop stabilizes the guanine-nucleotide exchange factor Cdc24 at sites of polarization. *EMBO J* **21:** 1565–1576

Butty AC, Pryciak PM, Huang LS, Herskowitz I, Peter M (1998) The role of Far1p in linking the heterotrimeric G protein to polarity establishment proteins during yeast mating. *Science* **282:** 1511–1516

Caviston JP, Longtine M, Pringle JR, Bi E (2003) The role of Cdc42p GTPase-activating proteins in assembly of the septin ring in yeast. *Mol Biol Cell* **14:** 4051–4066

Chang F, Peter M (2003) Yeasts make their mark. *Nat Cell Biol* **5:** 294–299

Drubin DG (2000) *Cell Polarity*. Oxford: Oxford University Press

Elion EA (1995) Ste5p: a meeting place for MAP kinases and their associates. *Trends Cell Biol* **5:** 322–327

Funk M, Niedenthal R, Mumberg D, Brinkmann K, Rönicke V, Henkel T (2002) Vector systems for heterologous expression of proteins in *Saccharomyces cerevisiae*. *Methods Enzymol* **350:** 248–257

Gladfelter AS, Bose I, Zyla TR, Bardes ES, Lew DJ (2002) Septin ring assembly involves cycles of GTP loading and hydrolysis by Cdc42p. *J Cell Biol* **156:** 315–326

Gulli MP, Jaquenoud M, Shimada Y, Niederhauser G, Wiget P, Peter M (2000) Phosphorylation of the Cdc42 exchange factor Cdc24 by the PAK-like kinase Cla4 may regulate polarized growth in yeast. *Mol Cell* **6:** 1155–1167

Guthrie C, Fink GR (1991) *Guide to Yeast Genetics and Molecular Biology*. San Diego, California, USA: Academic Press Inc.

Gyuris J, Golemis E, Chertkov H, Brent R (1993) Cdi1, a human G1 and S phase protein phosphatase that associates with Cdk2. *Cell* **75:** 791–803

Henchoz S, Chi Y, Catarin B, Herskowitz I, Deshaies RJ, Peter M (1997) Phosphorylation- and ubiquitin-dependent degradation of the cyclin-dependent kinase inhibitor Far1p in budding yeast. *Genes Dev* **11:** 3046–3060

Irazoqui JE, Gladfelter AS, Lew DJ (2003) Scaffold-mediated symmetry breaking by Cdc42p. *Nat Cell Biol* **5:** 1062–1070

Jaquenoud M, Peter M (2000) Gic2p may link activated Cdc42p to components involved in actin polarization, including Bni1p and Bud6p (Aip3p). *Mol Cell Biol* **20:** 6244–6258

Jaquenoud M, Gulli MP, Peter K, Peter M (1998) The Cdc42p effector Gic2p is targeted for ubiquitin-dependent degradation by the SCFGrr1 complex. *EMBO J* **17:** 5360–5373

Johnson DI (1999) Cdc42: an essential Rho-type GTPase controlling eukaryotic cell polarity. *Microbiol Mol Biol Rev* **63:** 54–105

Kang PJ, Sanson A, Lee B, Park HO (2001) A GDP/GTP exchange factor involved in linking a spatial landmark to cell polarity. *Science* **292:** 1376–1378

Kim YJ, Francisco L, Chen GC, Marcotte E, Chan CS (1994) Control of cellular morphogenesis by the Ip12/Bem2 GTPase-activating protein: possible role of protein phosphorylation. *J Cell Biol* **127:** 1381–1394

Levchenko A, Iglesias PA (2002) Models of eukaryotic gradient sensing: application to chemotaxis of amoebae and neutrophils. *Biophys J* **82:** 50–63

Marquitz AR, Harrison JC, Bose I, Zyla TR, McMillan JN, Lew DJ (2002) The Rho-GAP Bem2p plays a GAP-independent role in the morphogenesis checkpoint. *EMBO J* **21:** 4012–4025

McCusker D, Denison C, Anderson S, Egelhofer TA, Yates JR, Gygi SP, Kellogg DR (2007) Cdk1 coordinates cell-surface growth with the cell cycle. *Nat Cell Biol* **9:** 506–515

Moon SY, Zheng Y (2003) Rho GTPase-activating proteins in cell regulation. *Trends Cell Biol* **13:** 13–22

Nern A, Arkowitz RA (2000) Nucleocytoplasmic shuttling of the Cdc42p exchange factor Cdc24p. *J Cell Biol* **148:** 1115–1122

Ozbudak EM, Becskei A, van Oudenaarden A (2005) A system of counteracting feedback loops regulates Cdc42p activity during spontaneous cell polarization. *Dev Cell* **9:** 565–571

Peter M, Sanghera JS, Pelech SL, Nigg EA (1992) Mitogen-activated protein kinases phosphorylate nuclear lamins and display sequence specificity overlapping that of mitotic protein kinase p34cdc2. *Eur J Biochem* **205:** 287–294

Peterson J, Zheng Y, Bender L, Myers A, Cerione R, Bender A (1994) Interactions between the bud emergence proteins Bem1p and Bem2p and Rho-type GTPases in yeast. *J Cell Biol* **127:** 1395–1406

Pruyne D, Bretscher A (2000) Polarization of cell growth in yeast I: establishment and maintenance of polarity states. *J Cell Sci* **113:** 365–375

Rittinger K, Walker PA, Eccleston JF, Smerdon SJ, Gamblin SJ (1997) Structure at 1.65 Å of RhoA and its GTPase-activating protein in complex with a transition-state analogue. *Nature* **389:** 758–762

Shimada Y, Gulli MP, Peter M (2000) Nuclear sequestration of the exchange factor Cdc24 by Far1 regulates cell polarity during yeast mating. *Nat Cell Biol* **2:** 117–124

Shimada Y, Wiget P, Gulli MP, Bi E, Peter M (2004) The nucleotide exchange factor Cdc24p may be regulated by autoinhibition. *EMBO J* **23:** 1051–1062

Sikorski RS, Hieter P (1989) A system of shuttle vectors and yeast host strains designed for efficient manipulation of DNA in *Saccharomyces cerevisiae*. *Genetics* **122:** 19–27

Smith GR, Givan SA, Cullen P, Sprague Jr GF (2002) GTPase-activating proteins for Cdc42. *Eukaryot Cell* **1:** 469–480

Sohrmann M, Peter M (2003) Polarizing without a c(l)ue. *Trends Cell Biol* **13:** 526–533

Sopko R, Huang D, Smith JC, Figeys D, Andrews B (2007) Activation of the Cdc42p GTPase by cyclin-dependent protein kinases in budding yeast. *EMBO J* (in press)

Toenjes KA, Sawyer MM, Johnson DI (1999) The guanine-nucleotide-exchange factor cdc24p is targeted to the nucleus and polarized growth sites. *Curr Biol* **9:** 1183–1186

Ubersax JA, Woodbury EL, Quang PN, Paraz M, Blethrow JD, Shah K, Shokat KM, Morgan DO (2003) Targets of the cyclin-dependent kinase Cdk1. *Nature* **425:** 859–864

van Drogen F, Stucke VM, Jorritsma G, Peter M (2001) MAP kinase dynamics in response to pheromones in budding yeast. *Nat Cell Biol* **3:** 1051–1059

Wang T, Bretscher A (1995) The *rho*-GAP encoded by *BEM2* regulates cytoskeletal structure in budding yeast. *Mol Biol Cell* **6:** 1011–1024

Wedlich-Soldner R, Li R (2003) Spontaneous cell polarization: undermining determinism. *Nat Cell Biol* **5:** 267–270

Zhang B, Zhang Y, Collins CC, Johnson DI, Zheng Y (1999) A built-in arginine finger triggers the self-stimulatory GTPase-activating activity of rho family GTPases. *J Biol Chem* **274:** 2609–2612

Zheng Y, Cerione R, Bender A (1994) Control of the yeast bud-site assembly GTPase Cdc42. Catalysis of guanine nucleotide exchange by Cdc24 and stimulation of GTPase activity by Bem3. *J Biol Chem* **269:** 2369–2372

Zheng Y, Hart MJ, Shinjo K, Evans T, Bender A, Cerione RA (1993) Biochemical comparisons of the *Saccharomyces cerevisiae* Bem2 and Bem3 proteins. Delineation of a limit Cdc42 GTPase-activating protein domain. *J Biol Chem* **268:** 24629–24634